NEAREST-MANIFOLD CLASSIFICATION APPROACH FOR CARDIAC ARREST RHYTHM INTERPRETATION DURING RESUSCITATION

Ali Bahrami Rad[1], Trygve Eftestøl[1], Jan Terje Kvaløy[2], Unai Ayala[3],
Jo Kramer-Johansen[4], and Kjersti Engan[1]

[1] Department of Electrical Engineering and Computer Science, University of Stavanger, Norway
[2] Department of Mathematics and Natural Sciences, University of Stavanger, Norway
[3] Department of Communications Engineering, University of the Basque Country (UPV/EHU), Spain
[4] Norwegian Centre for Prehospital Emergency Care (NAKOS) and Institute for Clinical
Medicine, Oslo University Hospital and University of Oslo, Norway
ali.bahrami.rad@uis.no

ABSTRACT

In order to monitor the cardiac arrest patients response to therapy, there is a need for methods that can reliably interpret the different types of cardiac rhythms that can occur during a resuscitation episode. These rhythms can be categorized to five groups; ventricular tachycardia, ventricular fibrillation, pulseless electrical activity, asystole, and pulse generating rhythm. The objective of this study was to develop machine learning algorithms to automatically recognize these rhythms. We proposed a detection algorithm based on the nearest-manifold classification approach using a group of 8 time-domain features as statistical measures on the signal itself, as well as the first and second differences. The overall accuracy of the cardiac arrest rhythm interpretation is 79% which is 9% better than our prior work. The sensitivity/specificity of shockable/non-shockable rhythms is 92/95%.

Index Terms— Electrocardiogram, cardiac arrest rhythm interpretation, pattern recognition, K-nearest neighbors, nearest-manifold, K-local hyperplane distance nearest-neighbor

1. INTRODUCTION

During resuscitation of cardiac arrest victims professional rescuers provide chest compressions, ventilation, drugs and electrical shocks to the patient. The patient's response to this therapy can be evaluated through interpretation of the electrocardiogram (ECG) recorded during therapy. During resuscitation, even trained personnel may have high error rates [1], and this adds to the general quality issues reported from cardiac arrest treatment [2, 3].

Resuscitation data review has been important in the work of several resuscitation research groups [2, 4, 5]. Although the approaches for data review differs in many aspects, there are some fundamental similarities regarding rhythm interpretation and determining chest compression sequences. These review processes are also dependent on manual interpretation and registration which is time consuming and resource demanding.

We want to develop methods to facilitate efficient resuscitation data analysis. To achieve this it is important to provide reliable automatic methods for the fundamental parts of the review process. In this study, we focus on developing methods for automatic rhythm interpretation.

This work is organized as follows: Section 2 explains the cardiac arrest rhythms appearing during resuscitation episodes. In addition, the related prior work on cardiac arrest rhythm interpretation is discussed in this section. Section 3 describes the classification algorithm and feature extraction method. Sections 4 and 5 present the results and discussion.

2. CARDIAC ARREST RHYTHM INTERPRETATION

2.1. Cardiac arrest rhythms appearing during resuscitation episodes

In previous work involving manual review of resuscitation data, cardiac arrest rhythms appearing during resuscitation episodes has been categorized into five groups [2, 4]. The first rhythm is ventricular tachycardia (VT) which is a rapid heartbeat in which the heart does not pump blood efficiently due to inadequate filling and thus lower stroke volume. It is usually a temporary condition either spontaneously corrects or deteriorates into ventricular fibrillation. Ventricular fibrillation (VF) results in an unstable and irregular rapid heart rhythm. The electrical impulses travel chaotically through the myocardium and prevents proper heartbeat. The third rhythm is pulseless electrical activity (PEA) in which there exists an organized electrical activity in the heart, but there is no mechanical activity and thus palpable pulse. The fourth rhythm is asystole (AS) in which there is no significant electrical and mechanical activities. In addition to the above rhythms, the fifth category encompasses all pulse generating rhythms (PR). Fig. 1 shows examples from these five different categories.

In the context of shock advice algorithms, the first two rhythms (VT and VF) are considered shockable rhythms which is treatable using defibrillation, and the remaining three rhythms (PEA, AS, and PR) are considered non-shockable rhythms where defibrillation is not useful.

2.2. Relation to prior work

Historically, cardiac arrest rhythm analysis during resuscitation has been dedicated to detection of shockable and non-shockable rhythms in the development of so-called shock advice algorithms [6, 7]. Most of those algorithms consist of different sub-algorithms where each one tries to recognize different rhythms based on the emulation of expert judgment; for example detection of QRS for non-shockable
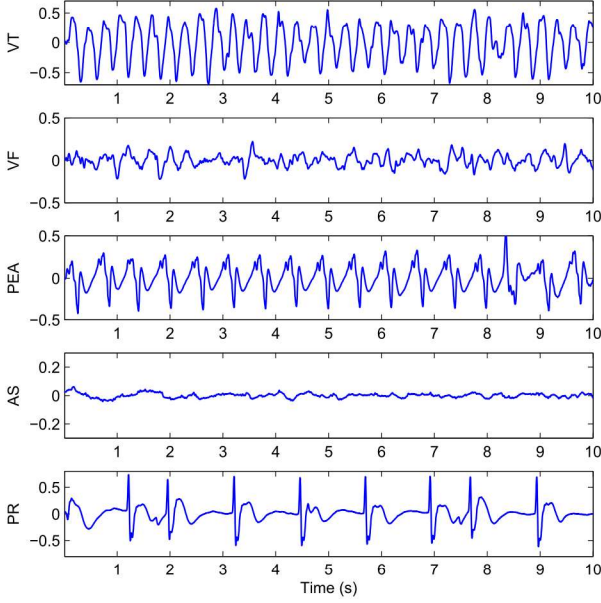
Fig. 1. Representation of the 10s segments of five different rhythm types (VT, VF, PEA, AS, and PR) during cardiac arrest. The y axes are the amplitudes of the ECG signals in mV which are shown in the different ranges for better representation.

rhythms [6]. Moreover, there are a few studies that have tried to distinguishing between other types of cardiac arrest rhythms; rhythm discrimination between PEA and PR has been proposed by [8].

Furthermore, in manual reviews it is common to consider all the cardiac rhythms during resuscitation (VT, VF, PEA, AS, PR) rather than just broad categories of shockable/non-shockable rhythms [9]; for further processing such as the evaluation of quality of CPR [2, 10] and analysis of state transition [4, 11, 12] the interpretation of all different types of cardiac rhythms are needed. To the best of our knowledge our previous study [13] was the first attempt to detect these five different cardiac rhythms in which we used a probabilistic framework with naïve Bayes (NB) and logistic regression classifiers with wavelet domain features.

The work presented here can be considered as a continuation of [13] in which we use a geometrical framework to address the rhythms interpretation problem. We used a nearest-manifold approach with time-domain features as described in section 3. After finding different rhythms it is easy to propose shock advice algorithms based on that. But, we should emphasize that the primary purpose of our study was/is to detect different rhythms. Shock advice can be considered a secondary objective.

3. NEAREST-MANIFOLD CLASSIFICATION APPROACH

Many real-world data sets are high-dimensional with non-uniform distributions which are concentrated around low-dimensional geometric structures. In other word, they are low-dimensional (linear or nonlinear) manifolds embedded within high-dimensional spaces. Discovering such structures so-called manifold learning has been investigated in the literature of dimensionality reduction over the last decade [14, 15, 16, 17, 18]. While the purpose of dimensionality reduction is to find the low-dimensional representation of data, there is another possibility to benefit from the manifold assumption of data; it can be used in the classification task.

Inspired by the K-nearest neighbors (KNN) classification method with the extra assumption that the data of each class is located on the low-dimensional manifold; we can classify a query sample to the closest manifold. One interpretation of this method is that the empty spaces in the KNN classification paradigm are virtually filled by the points located on the manifolds. But, since in general those manifolds do not have analytical expressions, computing distances from the query sample to them can be problematic. To address this problem, assuming that the manifolds of data sets are smooth, then a nonlinear manifold can be approximated as a set of locally linear manifolds. Thus, for finding the closest manifold to a query sample we need to find locally linear manifolds of different classes and then associate the class to the locally linear manifold which has the smallest distance to the query sample. This idea was introduced in [19] and named as K-local hyperplane distance nearest-neighbor algorithm (HKNN).

HKNN or extensions of it are applied successfully on several classification tasks ranging from bioinformatics to face recognition and image segmentation [20, 21, 22, 23, 24, 25]. In the following, at first we discuss HKNN algorithms in section 3.1, and then we describe the feature extraction in section 3.2.

3.1. K-local hyperplane distance nearest-neighbor algorithm

HKNN is a modified version of KNN in which for a given query point $\mathbf{x}$ we are looking for the closest local hyperplane in the neighborhood of $\mathbf{x}$ where each hyperplane belongs to a specific class $\mathcal{C}_m$ ($m = 1 \cdots M$ and M is the number of classes). To this end, in each class $\mathcal{C}_m$ we find the K nearest points to the query point, then find the hyperplane crossing those points, and finally find the minimum distance hyperplane to the query point.

Suppose $N_{\mathcal{C}_m}^K = \left\{ \mathbf{n}_1^{\mathcal{C}_m}, \mathbf{n}_2^{\mathcal{C}_m}, \cdots, \mathbf{n}_K^{\mathcal{C}_m} \right\}$ represents the set of K-nearest points to a query point $\mathbf{x}$ belonging to the $\mathcal{C}_m$ class, and $\bar{\mathbf{n}}^{\mathcal{C}_m} = \frac{1}{K} \sum_{k=1}^{K} \mathbf{n}_k^{\mathcal{C}_m}$ is the centroid of them. Then, the $\mathcal{C}_m$ local hyperplane can be expressed as

$$\mathrm{LH}_{\mathcal{C}_m}^K(\mathbf{x}) = \left\{ \bar{\mathbf{n}}^{\mathcal{C}_m} + \sum_{k=1}^{K} \alpha_k^{\mathcal{C}_m} \mathbf{v}_k^{\mathcal{C}_m} \middle| \alpha_{1 \cdots K}^{\mathcal{C}_m} \in \mathbb{R}^K \right\}, \quad (1)$$

where $\mathbf{v}_k^{\mathcal{C}_m} = \mathbf{n}_k^{\mathcal{C}_m} - \bar{\mathbf{n}}^{\mathcal{C}_m}$. The distance of $\mathbf{x}$ from this hyperplane is

$$d\left(\mathbf{x}, \mathrm{LH}_{\mathcal{C}_m}^K(\mathbf{x})\right) = \min_{\alpha_{1 \cdots K}^{\mathcal{C}_m} \in \mathbb{R}^K} \left\| \mathbf{x} - \bar{\mathbf{n}}^{\mathcal{C}_m} - \sum_{k=1}^{K} \alpha_k^{\mathcal{C}_m} \mathbf{v}_k^{\mathcal{C}_m} \right\|, \quad (2)$$

where $\|\cdot\|$ denotes the Euclidean norm. In order to determine $\alpha_k^{\mathcal{C}_m}$, we need to solve the linear system

$$(V_{\mathcal{C}_m}^T V_{\mathcal{C}_m}) \boldsymbol{\alpha}^{\mathcal{C}_m} = V_{\mathcal{C}_m}^T (\mathbf{x} - \bar{\mathbf{n}}^{\mathcal{C}_m}) \quad (3)$$

where $\mathbf{x}$ and $\bar{\mathbf{n}}^{\mathcal{C}_m}$ are D dimensional column vectors, $\boldsymbol{\alpha}^{\mathcal{C}_m} = (\alpha_1^{\mathcal{C}_m}, \cdots, \alpha_K^{\mathcal{C}_m})^T$, and $V_{\mathcal{C}_m}$ is a $D \times K$ matrix whose columns are the $\mathbf{v}_k^{\mathcal{C}_m}$ vectors. After finding the distances of $\mathbf{x}$ from all local hyperplanes, we can classify it in the following way

$$\mathcal{C}^* = \arg\min_{\mathcal{C}_m} d\left(\mathbf{x}, \mathrm{LH}_{\mathcal{C}_m}^K(\mathbf{x})\right). \quad (4)$$

In addition, a penalty term λ can be defined to penalize large values of $\alpha_k^{\mathcal{C}_m}$ (which corresponds moving away from centroid) in the following way

$$d'\left(\mathbf{x}, \mathrm{LH}_{\mathcal{C}_m}^K(\mathbf{x})\right)^2 =$$

$$\min_{\alpha_{1\cdots K}^{\mathcal{C}_m} \in \mathbb{R}^K} \left\| \mathbf{x} - \bar{\mathbf{n}}^{\mathcal{C}_m} - \sum_{k=1}^{K} \alpha_k^{\mathcal{C}_m} \mathbf{v}_k^{\mathcal{C}_m} \right\|^2 + \lambda \sum_{k=1}^{K} (\alpha_k^{\mathcal{C}_m})^2. \quad (5)$$

It should be noted that a hyperplane can approximate a class manifold only locally. Thus, it is reasonable that for points which are located far from centroid the hyperplane is no more a good approximation of the manifold. To determine $\alpha_k^{\mathcal{C}_m}$ in Eq. 5 this new linear system must be solved

$$(V_{\mathcal{C}_m}^T V_{\mathcal{C}_m} + \lambda \mathbf{I}) \boldsymbol{\alpha}^{\mathcal{C}_m} = V_{\mathcal{C}_m}^T (\mathbf{x} - \bar{\mathbf{n}}^{\mathcal{C}_m}), \quad (6)$$

where $\mathbf{I}$ is the $K \times K$ identity matrix. Finally, to classify the test data, in Eq. 4 the distance measure $d\left(\mathbf{x}, \mathrm{LH}_{\mathcal{C}_m}^K(\mathbf{x})\right)$ must be replaced by the new distance measure $d'\left(\mathbf{x}, \mathrm{LH}_{\mathcal{C}_m}^K(\mathbf{x})\right)$ defined by Eq. 5.

3.2. Feature extraction

After trying several different sets of features ranging from wavelet domain features as described in [13] to discrete cosine transform and time domain histogram, the best results were achieved using simple set of time domain features.

The features which are used in this study are 8 different statistical descriptors of the signal $s(n)$ and its first and second difference $\dot{s}(n) = s(n+1) - s(n)$, and $\ddot{s}(n) = \dot{s}(n+1) - \dot{s}(n)$ as follows:

The first three features are the interquartile ranges (which is the difference between the upper and lower quartiles) of $\mathbf{s}_N$, $\dot{\mathbf{s}}_N$, and $\ddot{\mathbf{s}}_N$ where $\mathbf{s}_N = (s(1), \cdots, s(\mathrm{N}))^T$, $\dot{\mathbf{s}}_N = (\dot{s}(1), \cdots, \dot{s}(\mathrm{N}-1))^T$, and $\ddot{\mathbf{s}}_N = (\ddot{s}(1), \cdots, \ddot{s}(\mathrm{N}-2))^T$. The next three features are related to the second, third, and forth statistics of the signal $\mathbf{s}_N$ as follows

$$|E\left[(\mathbf{s}_N - E\left[\mathbf{s}_N\right])^p\right]|^{1/p} \quad \text{for } p = 2, 3, 4 \quad (7)$$

where $E\left[(\mathbf{s}_N - E\left[\mathbf{s}_N\right])^p\right]$ is the p-th central moment of the signal $\mathbf{s}_N$, and $|\cdot|$ denotes the absolute value. The power $1/p$ is used in order to make the features in the same unit as the signal $\mathbf{s}_N$. In the initial tests, instead of third and fourth moments we used skewness and kurtosis which are dimensionless quantities, but it turns out that the above features are better. Finally, the last two features are related to the third, and forth statistics of the first difference signal $\dot{\mathbf{s}}_N$

$$|E\left[(\dot{\mathbf{s}}_N - E\left[\dot{\mathbf{s}}_N\right])^q\right]|^{1/q} \quad \text{for } q = 3, 4. \quad (8)$$

In addition to the above time domain (TD) features, for the comparison purpose we used the second set of features in the wavelet domain (WD) as described in [13].

4. EVALUATION

4.1. ECG database

The data used in this work was extracted from a large out-of-hospital cardiac arrest patients study. The original study was conceived to measure the CPR quality in three geographic locations between March 2002 and September 2004. A modified version of Laerdal's Heartstart 4000 defibrillator was used to record surface ECG. Episodes were annotated by expert reviewers using five

Table 1. The overall accuracy (Acc) of the cardiac arrest rhythm detection for 3s segments in addition to sensitivity (Sen) and specificity (Spe) of shockable and non-shockable rhythms.

Algorithm	Features	Acc	Sen	Spe
HKNN, $K = 6$, $\lambda = 0.5$	TD	79%	92%	95%
HKNN, $K = 13$, $\lambda = 200$	WD	75%	93%	96%
KNN, $K = 10$	TD	76%	95%	95%
KNN, $K = 5$	WD	71%	86%	95%
NB	TD	64%	97%	83%
NB	WD	70%	94%	90%

rhythm types (VF, VT, AS, PEA, and PR). For this study, artifact-free segments with a single rhythm type annotation and a duration of ten seconds (10s) were extracted. Records were resampled to 250 Hz. After reviewing the annotations a total of 1121 segments were included in the database, which is composed of 269 VF, 25 VT, 262 AS, 411 PEA, and 154 PR.

For training and testing the classifier we used exactly the same data as [13] in order to make the comparison of the results easier. For training the classifiers, approximately 75% of the ECG data is used. The training data consists of 176 VF, 15 VT, 214 AS, 311 PEA, and 115 PR. The remaining 25% of the ECG data is used as the test data set for evaluation of the performance of the classifiers. The test data consists of 93 VF, 10 VT, 48 AS, 100 PEA, and 39 PR.

4.2. Experiments and results

In order to test the accuracy of the proposed method, we have conducted experiments to classify all five rhythm categories (VF, VT, AS, PEA, and PR) based on both proposed method of this study (HKNN in addition to the ordinary KNN) and proposed method in the previous study (NB classifier) [13]. Although the purpose of this study was to classify those five rhythms, in order to compare the proposed method to shock advice algorithms we have also reported the sensitivity and specificity of shockable (VF+VT), and non-shockable (AS+PEA+PR) rhythms.

In our experiments two different sets of features TD and WD as described in section 3.2 are used. Both sets of features are normalized such that TD features lie in the interval $[0, 1]$ and WD features lie in the interval $[-1, 1]$. All reported results in this section refer to the test data set.

Table 1 shows the best performance, in the sense of the accuracy of rhythm detection for 3s segments of the ECG signals with different algorithms including HKNN, KNN, and NB for both TD and WD sets of features. In order to compare different methods in details, also the confusion matrices for the results of HKNN ($K = 6$, $\lambda = 0.5$, and TD features), KNN ($K = 10$ and TD features) and NB (WD features) are represented in Table 2. Finally, Fig. 2 demonstrates the accuracy of rhythm detection of HKNN and KNN methods for both TD and WD sets of features for different values of K (and λ in the case of HKNN).

5. DISCUSSION AND CONCLUSIONS

The results in Table 1 show a significant improvement in the accuracy of rhythm recognition; HKNN with TD features, $K = 6$, and $\lambda = 0.5$ has 79% accuracy which is 9% better than our previous work [13]. The sensitivity/specificity of shockable/non-shockable is 92/95%.

Table 2. The confusion matrices for HKNN ($K = 6$, $\lambda = 0.5$, and TD features), KNN ($K = 10$ and TD features) and NB (WD features) classification methods for 3s segments.

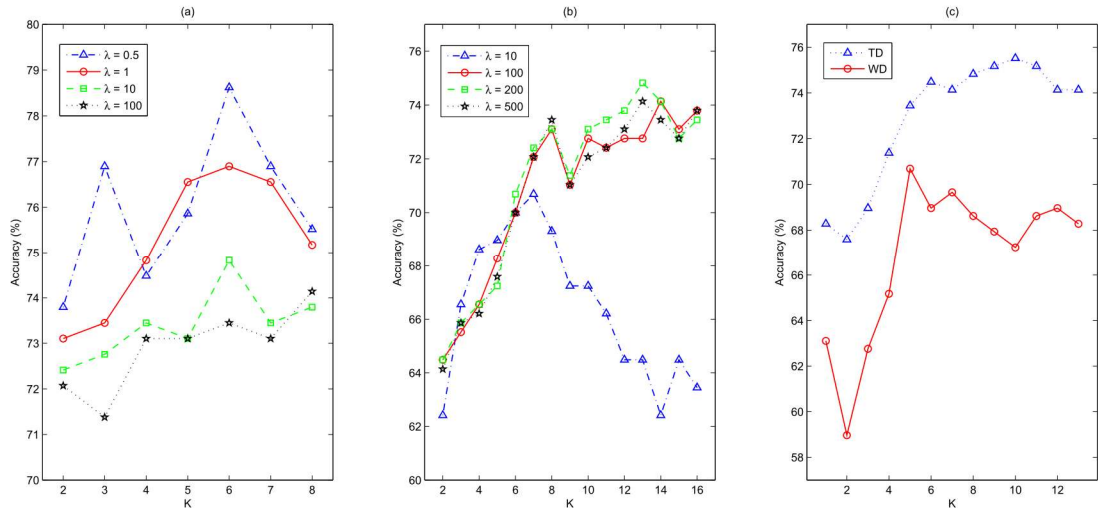|	HKNN					KNN					NB				
	AS	PEA	PR	VF	VT	AS	PEA	PR	VF	VT	AS	PEA	PR	VF	VT
AS	42	6	0	0	0	42	5	0	1	0	42	5	0	1	0
PEA	6	80	8	6	0	9	76	10	5	0	11	63	17	9	0
PR	1	18	17	3	0	0	24	11	4	0	0	8	22	5	4
VF	0	4	1	88	0	0	2	1	90	0	0	4	2	69	18
VT	0	3	0	6	1	0	1	1	8	0	0	0	0	4	6

Fig. 2. (a) demonstrates the accuracy of rhythm detection of HKNN with TD features for different values of K and λ. (b) shows the accuracy of rhythm detection of HKNN with WD features. And, (c) represents the accuracy of classification with KNN and both TD and WD features.

In all methods, most of the time the misclassification occurs within shockable/non-shockable categories, which means even if there are misclassifications in rhythm detection, usually shockable/non-shockable categories are detected correctly.

Although, the number of true PEA detection is significantly increased in the HKNN algorithm, PEA/PR detection still remains as the most problematic task in the context of cardiac arrest rhythm detection. By definition both PEA and PR classification represents organized cardiac rhythm and the only clinical differentiating feature is the palpable pulse. Pulse palpation as clinical test is notoriously difficult for both lay persons and professionals [26]. In the classification of clinical states in the original data set, the combination of ECG and CPR pattern and clinical notes from the patient report forms were used. Addition of more process information from the resuscitation episodes, such as content of CO_2 in the exhaled air (end tidal CO_2) or continuous oxymetry waveforms (SpO_2) could have aided the classification.

While the performance of VF detection is significantly increased, the performance of VT detection is not good due to the class imbalance problem. We are going to address this problem for HKNN algorithm in our future work.

In addition, it is worth pointing out that although the goal of introducing the parameter λ was to penalize the large values of $\alpha_k^{\mathcal{C}_m}$ in Eq. 5, the other possibility to benefit from the regularization parameter λ is that if in Eq. 5, the matrix $V_{\mathcal{C}_m}^T V_{\mathcal{C}_m}$ is ill-conditioned then by defining a non-zero value for λ the matrix $V_{\mathcal{C}_m}^T V_{\mathcal{C}_m} + \lambda\mathbf{I}$ will be well-conditioned and then Eq. 6 has reliable solution. In fact, with the sets of features we have chosen we have this problem. For example for HKNN with K = 6 as can be seen from Fig. 2-a the best results achieve with small value of $\lambda = 0.5$, but if we decrease λ further ($\lambda = 0$) then $V_{\mathcal{C}_m}^T V_{\mathcal{C}_m} + \lambda\mathbf{I}$ will be ill-conditioned. One possible remedy for this problem is that one use linear dimensionality reduction with PCA and find the direction related to the largest eigenvalues of $V_{\mathcal{C}_m}$ then find the hyperplane crossing them. This method will be investigated in our future work. Another suggestion is to design better feature extraction method.

One possible limitation of this work is that the results might be somewhat biased since we have not used k-folds cross validation method.

Finally, although in this study we achieve a significant improvement compare to the previous one, there is still room for further improvement possibly by the suggested approaches like better feature extraction method and extension of HKNN in the case of class imbalance problem.

6. REFERENCES

[1] J. Kramer-Johansen, D. P. Edelson, B. S. Abella, L. B. Becker, L. Wik, and P. A. Steen, "Pauses in chest compression and inappropriate shocks: A comparison of manual and semi-automatic defibrillation attempts," *Resuscitation*, vol. 73, no. 2, pp. 212–220, 2007.

[2] L. Wik, J. Kramer-Johansen, H. Myklebust, and et al., "Quality of cardiopulmonary resuscitation during out-of-hospital cardiac arrest," *JAMA*, vol. 293(3), pp. 299–304, 2005.

[3] B. S. Abella, "The importance of cardiopulmonary resuscitation quality," *Curr Opin Crit Care*, vol. 19, no. 3, pp. 175–180, 2013.

[4] T. Nordseth, D. Bergum, D. P. Edelson, T. M. Olasveengen, T. Eftestøl, R. Wiseth, B. S. Abella, and E. Skogvolla, "Clinical state transitions during advanced life support (ALS) in in-hospital cardiac arrest," *Resuscitation*, vol. 84, no. 9, pp. 1238–1244, 2013.

[5] T. D. Rea, R. E. Stickney, A. Doherty, and P. Lank, "Performance of chest compressions by laypersons during the public access defibrillation trial," *Resuscitation*, vol. 81, no. 3, pp. 293–296, 2010.

[6] U. Irusta, J. Ruiz, E. Aramendi, S. R. de Gauna, U. Ayala, and E. Alonso, "A high-temporal resolution algorithm to discriminate shockable from nonshockable rhythms in adults and children," *Resuscitation*, vol. 83, no. 9, pp. 1090–1097, 2012.

[7] V. Krasteva, I. Jekova, S. Menetre, T. Stoyanov, and J.-P. Didon, "Influence of analysis duration on the accuracy of a shock advisory system," in *Computing in Cardiology, 2011*, 2011, pp. 537–540.

[8] M. Risdal, S. O. Aase, J. Kramer-Johansen, and T. Eftestøl, "Automatic identification of return of spontaneous circulation during cardiopulmonary resuscitation," *Biomedical Engineering, IEEE Transactions on*, vol. 55, no. 1, pp. 60–68, 2008.

[9] T. Eftestøl and Sherman L. D., "Towards the automated analysis and database development of defibrillator data from cardiac arrest," *BioMed Research International*, vol. 2014, 2014.

[10] T. Eftestøl, K. A. H. Thorsen, E. Tøssebro, Rong C., and P. A. Steen, "Representing resuscitation data-considerations on efficient analysis of quality of cardiopulmonary resuscitation," *Resuscitation*, vol. 80, no. 3, pp. 311–317, 2009.

[11] E. Skogvoll, T. Eftestøl, K. Gundersen, J. T. Kvaløy, J. Kramer-Johansen, T. M. Olasveengen, and P. A. Steen, "Dynamics and state transitions during resuscitation in out-of-hospital cardiac arrest," *Resuscitation*, vol. 78, no. 1, pp. 30–37, 2008.

[12] J. T. Kvaløy, E. Skogvoll, T. Eftestøl, K. Gundersen, J. Kramer-Johansen, T. M. Olasveengen, and P. A. Steen, "Which factors influence spontaneous state transitions during resuscitation?," *Resuscitation*, vol. 80, no. 8, pp. 863–869, 2009.

[13] A. B. Rad, T. Eftestøl, J. T. Kvaløy, U. Ayala, J. Kramer-Johansen, and K. Engan, "Probabilistic classification approaches for cardiac arrest rhythm interpretation during resuscitation," in *Computing in Cardiology, 2013*, 2013.

[14] J. B. Tenenbaum, V. de Silva, and J. C. Langford, "A global geometric framework for nonlinear dimensionality reduction," *Science*, vol. 290, pp. 2319–2323, 2000.

[15] S. T. Roweis and L. K. Saul, "Nonlinear dimensionality reduction by locally linear embedding," *Science*, vol. 290, pp. 2323–2326, 2000.

[16] M. Belkin and P. Niyogi, "Laplacian eigenmaps and spectral techniques for embedding and clustering," in *Advances in Neural Information Processing Systems 14*. 2001, pp. 585–591, The MIT Press.

[17] D. L. Donoho and C. Grimes, "Hessian eigenmaps: Locally linear embedding techniques for high-dimensional data," *Proceedings of the National Academy of Sciences*, vol. 100, no. 10, pp. 5591–5596, 2003.

[18] R. R. Coifman and S. Lafon, "Diffusion maps," *Applied and Computational Harmonic Analysis*, vol. 21, no. 1, pp. 5–30, 2006.

[19] P. Vincent and Y. Bengio, "K-local hyperplane and convex distance nearest neighbor algorithms," in *Advances in Neural Information Processing Systems 14*. 2001, pp. 985–992, The MIT Press.

[20] O. Okun, "Protein fold recognition with k-local hyperplane distance nearest neighbor algorithm," in *Proceedings of the Second European Workshop on Data Mining and Text Mining in Bioinformatics*, 2004, vol. 1, pp. 51–57.

[21] L. Nanni and A. Lumini, "An ensemble of k-local hyperplanes for predicting protein-protein interactions," *Bioinformatics*, vol. 22, no. 10, pp. 1207–1210, 2006.

[22] Q. Ni, Z. Wang, and X. Wang, "Kernel k-local hyperplanes for predicting protein-protein interactions," in *Fourth International Conference on Natural Computation*, 2008, pp. 66–69.

[23] H. Cevikalp, D. Larlus, M. Neamtu, B. Triggs, and F. Jurie, "Manifold based local classifiers: Linear and nonlinear approaches," *Journal of Signal Processing Systems 61*, vol. 61(1), pp. 61–73, 2010.

[24] H. Cevikalp, B. Triggs, H. S. Yavuz, Y. Küçük, M. Küçük, and A. Barkana, "Large margin classifiers based on affine hulls," *Neurocomputing*, vol. 73, pp. 3160–3168, 2010.

[25] G. Wen, L. Jiang, J. Wen, J. Wei, and Z. Yu, "Perceptual relativity-based local hyperplane classification," *Neurocomputing*, vol. 97, pp. 155–163, 2012.

[26] B. Eberle, W. F. Dick, T. Schneider, G. Wisser, S. Doetsch, and I. Tzanova, "Checking the carotid pulse check: diagnostic accuracy of first responders in patients with and without a pulse," *Resuscitation*, vol. 33, no. 2, pp. 107–116, 1996.